

Dimerization of Pyrazole in Slit Jet Expansions

By Corey A. Rice, Nicole Borho, and Martin A. Suhm*

Institut für Physikalische Chemie, Universität Göttingen, Tammannstr. 6,
D-37077 Göttingen, Germany

Dedicated to Prof. Dr. Michael Buback on the occasion of his 60th birthday

(Received November 15, 2004; accepted November 23, 2004)

Jet FTIR / Hydrogen Bonds / Nanomatrices / Electron Correlation

Pyrazole dimer is observed for the first time in a free jet expansion. Its IR-active N–H stretching vibration is shifted by -269 cm^{-1} relative to the monomer. Along the 600 mm slit jet expansion, the average number density of pyrazole dimers is $\approx 10^{11}\text{ cm}^{-3}$. Exploratory quantum chemical calculations including electron correlation are in good agreement with the observed frequency shift and confirm reciprocal hydrogen bonding with bent hydrogen bonds in a planar C_{2h} structure, as postulated by W. Hückel 65 years ago in this journal. Nanomatrix isolation spectra can be obtained by using Ar as the carrier gas. The more strongly coupled vibrational dynamics in pyrazole trimer is illustrated.

1. Introduction

Considerable self-aggregation of molecules in the dilute gas phase is a rare phenomenon [1]. It only occurs in molecules with a pronounced hierarchy of intermolecular interactions. Strong, directed, and relatively unstrained hydrogen bonds have to be realized in “one-dimensional”, ring-like aggregates before weaker, non-directional attractions take over and lead to three-dimensional condensation [2]. The simplest and most pronounced case is hydrogen fluoride [2, 3], where hydrogen bonds stabilize cyclic oligomers consisting of about 4–6 monomers, whereas dispersion forces leading to three-dimensional condensation are weak. Small aliphatic alcohols such as methanol [1] also have some tendency for self-aggregation. In both cases, the hydrogen bond donor and acceptor sites in the monomers are separated by a single chemical bond (H–X). Due to this close vicinity, polarization can lead to pronounced non-additive contributions to the interaction strength. Another well-known case is carboxylic acids [4, 5], where three chemical bonds between the donor and

* Corresponding author. E-mail: msuhm@gwdg.de

acceptor atoms (H—O—C—O) provide for a strain-free dimer geometry and reduce non-additive contributions. Thus, there is no substantial driving force towards larger oligomers in this case and dimers dominate the vapor phase.

An interesting intermediate situation with *two* chemical bonds between donor and acceptor sites is offered by pyrazoles (H—N—N), derivatives of which are widely used in pharmaceutical and dye chemistry. Indeed, solid pyrazoles show a range of aggregation patterns ranging from C_{2h} dimers, C_{3h} trimers, and S_4 tetramers to chainlike and helical (catemer) arrangements, which react quite sensitively to chemical substitution at the aromatic ring ([6] and references therein). These aggregates of pyrazole ($C_3H_4N_2$) and many of its derivatives have been studied in much detail in solids, liquids, solutions, matrices, and in the gas phase, in particular by the group of Elguero [6]. An interesting and well studied dynamical phenomenon in the cyclic structures is concerted hydrogen tunneling with very large isotope effects [7, 8].

Despite a large number of studies, to the best of our knowledge no accurate experimental value of the IR-active N—H stretching vibration in the simplest aggregate of pyrazole itself, the pyrazole dimer, is available. This is surprising, because IR-spectroscopy is among the most sensitive probes of hydrogen bonding and the bathochromic N—H frequency shift upon dimerization is a quantity which is easily obtained from electronic structure calculations, at least in the harmonic approximation. There were early indications that cyclic trimers prevail in pyrazole solutions [9], whereas the C_{2h} dimer with its non-linear hydrogen bonds postulated by W. Hückel 65 years ago [10] is only a minor component under most conditions. In the crystal, the pyrazole units form hydrogen-bonded figure-of-eight spirals [11]. In the gas phase, IR absorptions attributed to the dimer of pyrazole have been observed along those of the monomer [12–14], but only at comparatively high temperatures, where inhomogeneous broadening renders a band center determination difficult. A strongly temperature-dependent band, peaking at 3280 to 3310 cm^{-1} , with a width of $\approx 100 \text{ cm}^{-1}$ was observed [12–14]. As thermal excitation tends to weaken the hydrogen bonds, the 0 K band center is expected at the low frequency end of this thermal band profile. The presence of non-negligible amounts of dimers in the equilibrium gas phase indicates that the acceptor quality of the aromatic π system is inferior to that of the in plane nitrogen lone pair.

Thermal excitation is also present in solution measurements [9], where the solvent shift renders a comparison to theory difficult, anyway. In a cryogenic matrix environment [12], the bands are more narrow, but the matrix shifts of both monomer and dimer again make a comparison to theoretical predictions difficult.

Supersonic jet spectroscopy is the method of choice to avoid both limitations. Due to the low vapor pressure of pyrazole, direct absorption measurements of expansions present a particular challenge. With the help of a new pulsed slit nozzle design [15] and a large vacuum buffer, we have succeeded

in obtaining jet-FTIR absorption spectra of pyrazole. In this contribution, we present the first unperturbed low-temperature N–H stretching transition of pyrazole dimer as a simple prototype of reciprocal hydrogen bonding and we demonstrate the matrix shifts induced by coating the monomers and dimers with Ar atoms. The experimental results are compared to exploratory quantum chemical predictions. Available computational results in the literature [7, 14] concentrate on hydrogen transfer or on derivatives of pyrazole.

2. Methods

Supersonic jet IR-spectra of the N–H stretching vibrations of pyrazole and its dimer seeded in He and Ar were recorded using the new filet jet-FTIR technique [15]. In brief, a giant gas pulse of up to 5 mol per second is expanded through a 600×0.2 mm slit nozzle into a 23 m^3 buffer chamber and probed perpendicularly by a single 2 cm^{-1} resolution scan of a Bruker Equinox 55 FTIR spectrometer. It is equipped with a tungsten source, a CaF_2 -beamsplitter and an optical filter ($2.5\text{--}3.5 \mu\text{m}$). The collimated IR-beam is focused and recollimated with two CaF_2 lenses of 500 and 250 mm focal length inside the jet chamber. A large area InSb detector is located in an external, evacuated detector chamber.

The gas expansion of 135 ms duration is controlled via six fast responding magnetic valves of 8 mm nominal width (Parker Lucifer) in combination with a pulse generator (BNC, Model 400). The “*fine, but lengthy*” (*filet*) jet expansion geometry optimizes monomer and dimer concentrations. In comparison to the previous ragout jet-FTIR [16] setup (120×0.5 mm), the formation of larger aggregates is reduced. The vacuum buffer is pumped by a series of roots blowers at $2000 \text{ m}^3 \text{ h}^{-1}$. After a recovery period of up to 120 s, the process is repeated and the resulting spectra are coadded. The gas mixtures are prepared by flowing He ($\geq 99.996\%$, Messer) at 2.5 bar or Ar ($\geq 99.998\%$, Messer) at 1.8 bar through a glass or stainless steel saturator containing solid pyrazole (98%, Lancaster) at 293 K. The stagnation pressure in the reservoir is 2.0 bar for He and 1.5 bar for Ar.

After each probe scan, there is a post-probe scan, which monitors the background gas ≈ 0.1 s after the breakdown of the expansion. Initially, the local pressure in the jet chamber is significantly higher than that in the total buffer volume. The post-probe scan allows for a quick comparison of the jet cooled spectrum and the gas phase, where clusters are absent. To explore the spectra of larger pyrazole clusters, ragout jet-FTIR spectra have also been recorded [5] (see Fig. 2). Their detailed analysis is beyond the scope of the present contribution.

Gaussian03 [17] was used to calculate pyrazole monomer, dimer, and trimer vibrational spectra at a range of electron correlation levels and basis sets. The levels of theory used were HF, B3LYP and MP2 with the 6-31+G(d),

Table 1. Calculated electronic (D_e /(kJ mol⁻¹)) and zero-point-corrected binding energies (D_0 /(kJ mol⁻¹)) of pyrazole dimer relative to two monomers.

D_e/D_0	6-31G(d)	6-31+G(d)	6-311+G(d,p)	6-311++G(d,p)	aug-cc-pVDZ
HF	45.4 [6]/-	41.5/36.1	40.5/35.3	40.5/35.2	38.4/33.1
B3LYP		50.5/45.1	51.2/46.1	51.1/46.0	50.6/45.1
MP2		65.9/61.6	64.7/61.2	-/-	69.2/64.8

6-311+G(d,p), 6-311++G(d,p), and aug-cc-pVDZ basis sets. Symmetry was used for the monomer (C_s), dimer (C_{2h}), and trimer (C_{3h}) and the absence of imaginary frequencies supported the minimum character of these structures. We note that some of the out-of-plane modes are relatively low in frequency, occasionally leading to spurious imaginary frequencies (*e.g.* at MP2/6-311++G(d,p) level). The trimer was only calculated using the B3LYP approach and the four different basis sets.

3. Results and discussion

Electronic structure calculations for pyrazole dimer were carried out for a range of levels and basis sets. The resulting dissociation energies relative to two monomers are listed in Table 1. Evaluation of the basis set superposition error (BSSE) indicates a contribution of $\approx 15\%$ – 20% to the binding energy. The zero point energy correction to the dimerization energy only amounts to about 5 kJ mol⁻¹ for this relatively heavy molecule. This is less than 10% of the binding energy at 0 K, which may be roughly estimated at 55 ± 10 kJ mol⁻¹ based on Table 1. Considering the bent geometry of the hydrogen bonds, this is a rather large value, comparable to that in carboxylic acid dimers [5]. At Hartree–Fock level, the hydrogen bond strength is underestimated, as expected. This is the only level at which a literature value for a full geometry optimization is available [6], to the best of our knowledge. However, several calculations at constrained geometries have been published [7] and come to qualitatively similar conclusions. The calculated dissociation energy for the trimer (*e.g.* $D_e = 109$ kJ mol⁻¹, $D_0 = 100$ kJ mol⁻¹ at B3LYP/6-311++G(d,p) level for dissociation into three monomers) is approximately 40%–50% higher than that of the dimer, on a per monomer basis. This is mostly due to the release of ring strain. However, with an estimated value of 40 ± 10 kJ mol⁻¹, the trimer dissociation energy per monomer unit still falls short of the evaporation enthalpy of 74.0 ± 0.4 kJ mol⁻¹ [18]. This shows that secondary interactions between monomer units provide non-negligible contributions to the cohesion energy of the solid.

The hydrogen bond strength is reflected in the bathochromic shift of the N–H stretching frequency upon aggregation. Table 2 lists calculated harmonic

Table 2. Harmonic wavenumbers ω/cm^{-1} for the IR-active N–H stretching mode in pyrazole monomer, dimer and trimer at various levels of theory. Also given are the corresponding integrated band strengths $A/\text{km mol}^{-1}$.

level	C_s monomer		C_{2h} dimer		C_{3h} trimer	
	ω cm^{-1}	A km mol^{-1}	ω cm^{-1}	A km mol^{-1}	ω cm^{-1}	A km mol^{-1}
HF/6-31+G(d)	3928	114	3821	952	–	–
HF/6-311+G(d,p)	3914	122	3794	1012	–	–
HF/6-311++G(d,p)	3915	122	3794	1014	–	–
HF/aug-cc-pVDZ	3916	116	3802	981	–	–
B3LYP/6-31+G(d)	3665	76	3444	1473	3263	2131
B3LYP/6-311+G(d,p)	3665	88	3412	1630	3189	2761
B3LYP/6-311++G(d,p)	3665	88	3410	1640	3189	2765
B3LYP/aug-cc-pVDZ	3660	83	3401	1691	3164	2924
MP2/6-31+G(d)	3667	99	3445	1458	–	–
MP2/6-311+G(d,p)	3679	100	3426	1618	–	–
MP2/aug-cc-pVDZ	3666	94	3371	1859	–	–

wavenumbers for the monomer, the C_{2h} dimer, and the C_{3h} trimer of pyrazole. Only the values for the IR-active mode are given. In agreement with the energetical findings, the hydrogen bond induced red shifts are considerably smaller at HF level than at levels including electron correlation. The B3LYP results for the trimer suggest that pyrazole dimer and trimer can be easily distinguished in the IR spectrum, as their predicted red shifts differ by almost a factor of two. This is partly a consequence of the more linear hydrogen bonds in the trimer [14].

Also listed in Table 2 are calculated band strengths, which increase by about one order of magnitude upon hydrogen bond formation, if divided by the number of N–H oscillators which are involved. Again, the HF enhancements are less pronounced. Similar results and conclusions have been previously obtained by Castaneda *et al.* [14] for 3,5-dimethylpyrazole at B3LYP and MP2 levels.

Because of the sizeable anharmonicity of the N–H stretching mode, comparison to experiment is better made for harmonic wavenumber *shifts*. For moderately strong hydrogen bonds and on an absolute scale, the effect of hydrogen bonding on anharmonic corrections is typically much smaller than that on harmonic wavenumbers. Table 3 summarizes the theoretical wavenumber shift predictions. MP2 shifts are systematically larger than B3LYP shifts, in contrast to the findings for H–F and O–H stretching vibrations. However, the differences are not large and well within the expected error bar at these levels of calculation. Considering that the B3LYP/aug-cc-pVDZ prediction for the trimer red shift is 496 cm^{-1} (Table 2), any experimental N–H shift below 350 cm^{-1} is likely to be due to pyrazole dimer, not trimer.

Table 3. Calculated red shifts $-\Delta\omega = \omega_M - \omega_D$ (in cm^{-1}) for the IR active harmonic N–H stretching wavenumber in the dimer (D) relative to the monomer (M) at various levels of theory combined with a range of basis sets. Also shown is the experimental anharmonic value.

level/ basis set	6-31+G(d)	6-311+G(d,p)	6-311++G(d,p)	aug-cc-pVDZ	experiment
HF	107	120	121	114	
B3LYP	221	253	255	259	
MP2	222	253	–	295	
anharmonic					269

At this stage, we can turn to the experimental IR spectra, which are shown in Fig. 1. The lower trace shows the gas phase spectrum in the range from 3600 to 3000 cm^{-1} as obtained ≈ 0.1 s after the end of the gas pulse into the vacuum chamber. Weak aromatic C–H stretching bands can be seen, but the spectrum is dominated by the hybrid band profile of the monomer N–H stretching band located around 3524 cm^{-1} . This band has been discussed in detail before [12, 13] and has been located more accurately at 3523.2 cm^{-1} [13]. In the jet expansion using He as the carrier gas (trace b), the pyrazole is cooled to low (≈ 20 K) rotational temperatures and the band profile narrows down considerably and is consistent with the monomer rotational constants.

To the red of the monomer band, the jet spectrum exhibits a narrow (≈ 6 cm^{-1} wide) new band, not present in the gas phase, at 3255 cm^{-1} . Based on its 269 cm^{-1} red shift relative to the monomer and on comparison to Table 3, it is due to the IR active N–H stretching vibration of the C_{2h} pyrazole dimer. The trimer band would be expected near to or below the C–H stretching modes. Ragout jet-FTIR spectra between 3400–2600 cm^{-1} (Fig. 2) indeed reveal a complex band pattern, which most likely includes the trimer and possibly larger clusters. The center of gravity of the large cluster absorptions is slightly shifted to the blue of the strong doublet, between 2900 and 3000 cm^{-1} . This is not too far from the expected trimer N–H stretching band center (Table 2). In line with the expectations for the fine slit of the file jet (Fig. 2), trimer formation is discouraged at the low monomer concentrations, which we estimate near 0.001% in He. Based on calculated band strengths, we can estimate an average number density of 10^{11} dimers per cm^3 with He as the carrier gas, $\approx 2\%$ of the monomer number density. The average number density for Ar as the carrier gas is about half that of He in Fig. 1.

It is instructive to discuss the broad thermal pyrazole dimer bands [12–14] in the context of the present reliable band center of 3255 cm^{-1} . Castaneda *et al.* [14] observed a broad band maximum at 3300 cm^{-1} at 460 K. Its low wavenumber *onset* around 3250 cm^{-1} is quite consistent with our band center and the width is clearly due to inhomogeneous (thermal) broadening. Similarly, Tabacik *et al.* [12] observed a band maximum at 3310 cm^{-1} at 408 K.

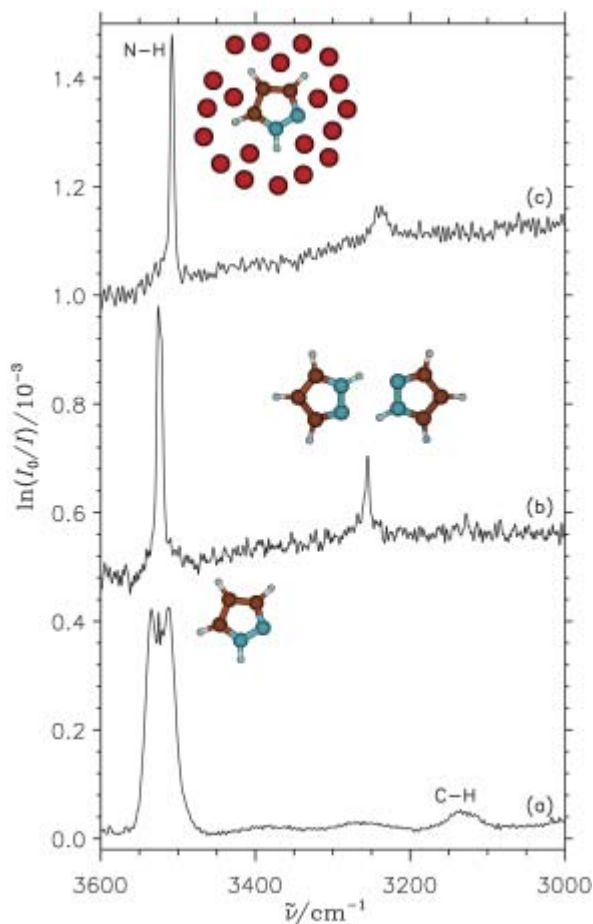


Fig. 1. NH/CH stretching region of the IR spectrum of pyrazole (a) in the gas phase ($\times 0.1$), (b) in the filet jet expansion (723 gas pulses, 2 bar, $\approx 0.001\%$) with helium as the carrier gas and (c) in the filet jet expansion (524 gas pulses, 1.5 bar, $\approx 0.001\%$) with argon as the carrier gas. Also shown are cartoons of pyrazole monomer (a), dimer (b) and Ar-coated monomer (c).

Majoube [13] observed a more narrow band with similar onset peaking around 3280 cm^{-1} at room temperature, again consistent with our observation. Thus, pyrazole dimer provides a good illustration of the inhomogeneous broadening and simultaneous blue shifting of hydrogen bonded X–H stretching modes with increasing temperature, a straightforward consequence of thermal weakening.

The B3LYP and MP2/aug-cc-pVDZ harmonic red shift predictions bracket the experimentally observed anharmonic shift. To some extent, this is clearly

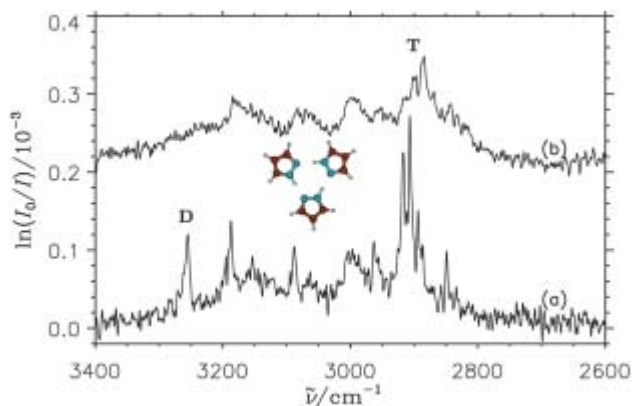


Fig. 2. NH/CH stretching region of the IR spectrum of pyrazole ($\approx 0.001\%$) between $3400\text{--}2600\text{ cm}^{-1}$, obtained by ragout jet-FTIR spectroscopy using (a) helium (198 gas pulses, 1.5 bar), and (b) argon (390 gas pulses, 1.5 bar) as the carrier gases. The dimer absorption (D) from Fig. 1 is marked. Due to the increased slit width, the spectrum shows extended resonance structures from larger clusters (T), most likely dominated by trimers.

fortuitous and it will be interesting to test the convergence of the theoretical predictions using higher levels of theory, also including anharmonic contributions. However, this is beyond the scope of this work.

Rather, we wish to establish a link to the existing bulk matrix isolation work on this system [12]. For this purpose, trace c of Fig. 1 shows the spectrum of a jet expansion of pyrazole in Ar (including Savitzky–Golay 25-point smoothing). The appearance is quite similar to that of the He expansion, but both the monomer and dimer absorptions are shifted to lower wavenumber. The monomer band, which is now more symmetric and more narrow, is located at 3508 cm^{-1} , 16 cm^{-1} to the red of the He-expansion. The dimer band has broadened and is red-shifted by 15 cm^{-1} to $\approx 3240\text{ cm}^{-1}$. We interpret the two bands as being due to Ar-coated pyrazole monomers and dimers, like in previous ragout jet-FTIR studies [5, 16]. This assignment is strongly supported by a comparison to the former bulk matrix study [12], which observed the monomer at 3507 cm^{-1} and a weak “ $\nu(\text{NH})$ assoc.” band at 3240 cm^{-1} . Thus, we can switch between free and nanomatrix-isolated molecules and clusters by simply changing the carrier gas in the file jet expansion. The nearly unchanged red shift of the dimer in the matrix environment is consistent with a robust hydrogen bonding situation in pyrazole dimer.

The spectral pattern observed for the trimer and possibly for larger clusters in the wider ragout jet expansion (Fig. 2) is strongly reminiscent of the situation in carboxylic acid dimers (see [5] and references cited therein). It is also seen in bulk phase studies of pyrazole [14], although in much less detail. Upon coating with Ar (trace b), some of the spectral detail is also lost in the jet. The

essential pattern persists, slightly shifted to lower wavenumber. This suggests that cluster isomerism is not the main reason for the spectral complexity. Due to the stronger N–H red-shift in the trimer, monomer framework modes are shifted into resonance with the N–H stretch, leading to a complex coupling scenario [19]. An important result of the present work is that this coupling is only switched on beyond the dimer.

4. Conclusions and outlook

We have presented filet jet-FTIR spectra of pyrazole monomers and dimers both free and within an argon nanomatrix environment. The agreement with exploratory quantum chemical calculations and bulk matrix spectra for the biologically important N–H chromophore is surprisingly good. In contrast to the solid state, where bulky 3,5-substituents (t-Bu, Ph) are needed to stabilize a pyrazole dimer structure [6], no significant amounts of larger clusters are observed in our dilute pulsed expansions through a 0.2 mm slit orifice. With the availability of an accurate IR active pyrazole dimer N–H stretching band center at 3255 cm^{-1} and a bathochromic shift of 269 cm^{-1} , accurate quantum chemical calculations including anharmonic contributions should now be carried out for this important prototype of reciprocal hydrogen bonding and proton tunneling [7, 8], which was first postulated by W. Hückel in 1940 [10]. This will also help in establishing reliable predictions for the more complicated cyclic trimer and crystal chain spectra, which involve extended Fermi resonance patterns [14, 20] like in many strongly hydrogen-bonded clusters built from organic molecules [5, 19]. A better description of pyrazole self-association may also be helpful for understanding the role of pyrazole in mixed complexes [14, 21] and in supramolecular design [22].

Acknowledgement

We thank C. Emmeluth, A. Warhausen, D. Luckhaus and U. Schmitt for help and discussions. We owe our gratitude to the machine shop crew for the construction of the filet jet nozzle. Support by the Deutsche Forschungsgemeinschaft via SFB 357 (Molekulare Mechanismen Unimolekularer Prozesse) and GRK 782 (www.pcgg.de) as well as by the Fonds der Chemischen Industrie is gratefully acknowledged.

References

1. W. Weltner, Jr. and K. S. Pitzer, *J. Am. Chem. Soc.* **73** (1951) 2606.
2. M. A. Suhm, *Ber. Bunsenges. Phys. Chem.* **99** (1995) 1159.
3. M. Quack and M. A. Suhm, *Spectroscopy and Quantum Dynamics of Hydrogen Fluoride Clusters*. In: J. M. Bowman and Z. Bačić (Eds.), *Molecular Clusters. Advances in Molecular Vibrations and Collision Dynamics*, Vol. III, JAI Press, London (1998).

4. E. M. Borschel and M. Buback, *Z. Naturforsch. A* **43** (1988) 207.
5. T. Häber, U. Schmitt, C. Emmeluth, and M. A. Suhm, *Faraday Discuss. Chem. Soc.* **118** (2001) 331 + contributions to the discussion on pp. 53, 119, 174–175, 179–180, 304–309, 361–363, 367–370.
6. C. Foces-Foces, I. Alkorta, and J. Elguero, *Acta Cryst. B* **56** (2000) 1018.
7. J. L. G. de Paz, J. Elguero, C. Foces-Foces, A. L. Llamas-Saiz, F. Aguilar-Parrilla, O. Klein, and H. H. Limbach, *J. Chem. Soc., Perkin Trans. 2* (1997) 101.
8. S. Schweiger and G. Rauhut, *J. Phys. Chem. A* **107** (2003) 9668.
9. D. M. W. Anderson, J. L. Duncan, and F. J. C. Rossotti, *J. Chem. Soc.* (1961) 140.
10. W. Hückel, J. Datow, and E. Simmersbach, *Z. Phys. Chem.* **186** (1940) 129.
11. F. K. Larsen, M. S. Lehmann, I. Sjøtofte, and S. E. Rasmussen, *Acta Chem. Scand.* **24** (1970) 3248.
12. V. Tabacik, V. Pellegrin, and H. H. Günthard, *Spectrochim. Acta Part A* **35** (1979) 1055.
13. M. Majoube, *J. Phys. Chem.* **92** (1988) 2407.
14. J. P. Castaneda, G. S. Denisov, S. Y. Kucherov, V. M. Schreiber, and A. V. Shurukhina, *J. Mol. Struct.* **660** (2003) 25.
15. N. Borho, M. A. Suhm, 2005 to be published.
16. T. Häber, U. Schmitt, and M. A. Suhm, *Phys. Chem. Chem. Phys.* **1** (1999) 5573.
17. M. J. Frisch, G. W. Trucks, H. B. Schlegel, G. E. Scuseria, M. A. Robb, J. R. Cheeseman, V. G. Zakrzewski, J. A. Montgomery, Jr., R. E. Stratmann, J. C. Burant, S. Dapprich, J. M. Millam, A. D. Daniels, K. N. Kudin, M. C. Strain, O. Farkas, J. Tomasi, V. Barone, M. Cossi, R. Cammi, B. Mennucci, C. Pomelli, C. Adamo, S. Clifford, J. Ochterski, G. A. Petersson, P. Y. Ayala, Q. Cui, K. Morokuma, D. K. Malick, A. D. Rabuck, K. Raghavachari, J. B. Foresman, J. Cioslowski, J. V. Ortiz, B. B. Stefanov, G. Liu, A. Liashenko, P. Piskorz, I. Komaromi, R. Gomperts, R. L. Martin, D. J. Fox, T. Keith, M. A. Al-Laham, C. Y. Peng, A. Nanayakkara, C. Gonzalez, M. Challacombe, P. M. W. Gill, B. Johnson, W. Chen, M. W. Wong, J. L. Andres, C. Gonzalez, M. Head-Gordon, E. S. Replogle, J. A. Pople *et al.*, *Gaussian 03* (Revision B.04), Gaussian Inc., Pittsburg PA, 2003.
18. P. Jiménez, M. V. Roux, C. Turrión, and F. Gomis, *J. Chem. Thermodyn.* **19** (1987) 985.
19. C. Emmeluth, M. A. Suhm, and D. Luckhaus, *J. Chem. Phys.* **118** (2003) 2242.
20. A. Zecchina, L. Cerruti, S. Coluccia, and E. Borello, *J. Chem. Soc. (B)* (1967) 1363.
21. C. Unterberg, A. Gerlach, T. Schrader, and M. Gerhards, *Eur. Phys. J. D* **20** (2002) 543.
22. I. Boldog, E. B. Rusanov, J. Sieler, S. Blaurock, K. V. Domasevitch, *Chem. Commun.* (2003) 740.